

# Recovering Temporal PSF using ToF Camera with Delayed Light Emission

Kazuya Kitano<sup>1,a)</sup> Takanori Okamoto<sup>1</sup> Kenichiro Tanaka<sup>1</sup> Takahito Aoto<sup>1</sup>  
Hiroyuki Kubo<sup>1</sup> Takuya Funatomi<sup>1</sup> Yasuhiro Mukaigawa<sup>1</sup>

## 1. Introduction

In recent years, the temporal Point Spread Function (PSF) of a scene, which is a response of the temporal impulsive light, is attracting attention because the propagation of light can be visualized. The temporal PSF conveys optical properties of the object hence it has broad potential applications such as inter-reflection and scattering analyses.

Temporal PSF of a scene can be obtained using an interferometer [1], holography [4], and femtosecond-pulsed laser [8], which require complex optics and expensive devices. Heide *et al.* [2] firstly recover a temporal PSF in an inexpensive way using an amplitude modulated continuous wave ToF camera. Using a continuous wave ToF camera, the light transport in units of nanoseconds can be visualized [3], [5], [6].

In this paper, we propose a method for estimating the temporal PSF using a *pulsed* ToF camera. Using pulsed ToF cameras, low temporal resolution PSFs can be straightforwardly obtained, *e.g.*, tens of nanoseconds, which is insufficient for analyzing scattering that is finished within 1 nanosecond. To achieve sub-nanoseconds resolution, we introduce an additional circuit for delaying the light emission. By delaying the light emission in sub-nanoseconds and obtain many observations, we recover temporal PSFs via computation and achieve sub-nanoseconds resolution.

Our contributions are twofold. Firstly, the PSF of the scene can be estimated even with the pulsed ToF camera. Secondly, we achieve sub-nanoseconds resolution temporal PSF. We show a simple PSF recovery technique by delaying the light emission and computation.

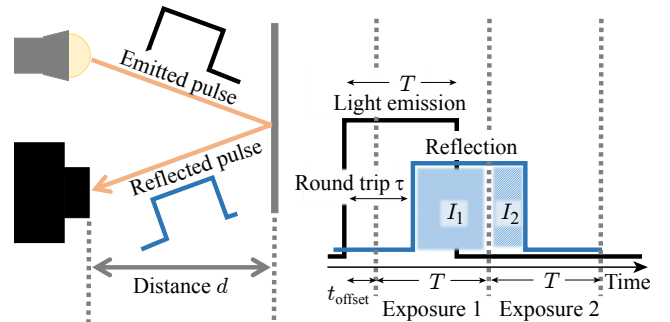


Fig. 1 Principle of ToF camera operation.

## 2. PSF estimation using ToF camera

In this section, we explain the method that estimates temporal PSF using pulsed ToF camera.

### 2.1 Principle of ToF camera operation

Originally, a ToF camera is a device for distance estimation by measuring the round trip time between the light emission and reflecting back to the camera. The distance to the object  $d$  is obtained as

$$d = \frac{c\tau}{2}, \quad (1)$$

where  $\tau$  is the measured round trip time and  $c$  is the speed of light. Because the observation of the ToF camera is independent for each pixel, the camera pixel  $p$  is omitted for simplicity. In this paper, we assume a pulsed ToF camera, which emits a square pulsed light for a few tens of nanoseconds as shown in Fig. 1. Synchronizing with the light emission, two images  $I_1$  and  $I_2$ , whose exposure time is the same as the width of the light emission, are obtained. From these two images, the round trip time  $\tau$  can be obtained as

$$\tau = \frac{I_2}{I_1 + I_2} T, \quad (2)$$

where  $T$  is the width of light emission and exposure.

<sup>1</sup> Nara Institute of Science and Technology

<sup>a)</sup> kitano.kazuya.jy9@is.naist.jp

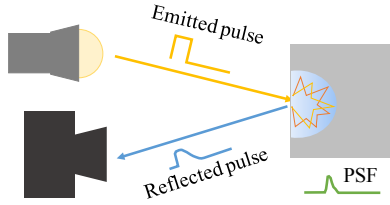


**Fig. 2** Waveform of the reflection is distorted due to subsurface scattering.

Moreover, because the observable range of the depth is limited to the width of the square wave, the start of the exposure is shifted to change the region of interest. In such a case, Eq. (2) can be written as

$$\tau = \frac{I_2}{I_1 + I_2}T + t_{\text{offset}}, \quad (3)$$

where  $t_{\text{offset}}$  is the shift of the exposure.

## 2.2 Distortion of reflected light due to PSF

The reflected light is assumed to be an ideal square wave in principle. However, in practice, the waveform of the reflection light is distorted according to the geometrical and optical characteristics of the scene as shown in Fig. 2. For example, if the scene includes objects that has subsurface scattering or inter-reflection occur, the temporal PSF  $r(t)$  of the scene is spread along with the time domain, therefore the waveform of the reflected light is no longer the square wave.

The reflection waveform reaching the ToF camera can be represented by the convolution of the emission wave  $l(t)$  and the temporal PSF  $r(t)$ . Observation  $i$  of the ToF camera is then represented as

$$i = \int g(s) (l \otimes r(s)) ds, \quad (4)$$

where  $\otimes$  is the convolution operator,  $s$  is an integral variable on the time domain, and  $g(t)$  is the function of the ToF camera representing the exposure sensitivity at a certain time  $t$ . We assume that  $g(t)$  takes a binary value, whether the sensor is exposed or not, however in general it can take a continuous value. The temporal spread by the optical system is ignored because it is sufficiently smaller than the ToF camera operation.

## 2.3 PSF estimation with delayed light emission

If the emission and exposure of the ToF camera can be freely controllable, the temporal PSF of the scene could be easily obtained. By infinitesimally shortening the light emission and exposure widths, the impulsive light emission  $l(t)$  and the exposure  $g(t)$  can be regarded as the

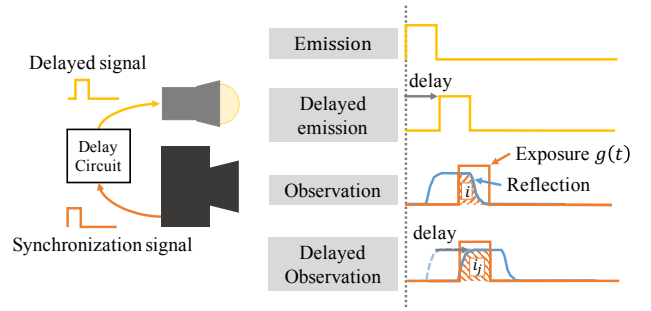


**Fig. 3** Light emission is delayed by an inserted circuit between the camera and the light source. Delayed light emission is equivalent to reversely shifting the exposure.

Dirac's delta function  $\delta(t)$ . The value of the temporal PSF  $r(t_j)$  at the exposure shift  $t_j$  is obtained as

$$r(t_j) = \int \delta(s - t_j) ((\delta \otimes r)(s)) ds. \quad (5)$$

Appropriately shifting the start of the exposure, the full temporal PSF  $r(t)$  can be directly obtained. However, it is difficult to infinitesimally shorten the emission and exposure width because of the limitation of the logical gates. Typical ToF cameras can only achieve in tens of nanoseconds resolution.

Even if the light emission and exposure width cannot be shortened, the PSF can be recovered from observations with shifting the exposure. The observation  $i(t_j)$  at the exposure shift  $t_j$  is represented as

$$\begin{aligned} i(t_j) &= \int g(s - t_j) (l \otimes r(s)) ds \\ &= g^* \otimes l \otimes r(t_j), \end{aligned} \quad (6)$$

where  $g^*$  is a exposure function whose time axis is inverted. By shifting the exposure finely, a *blurred* PSF  $i(t)$  can be observed. When the illumination  $l(t)$  and exposure  $g(t)$  are known, the original PSF  $r(t)$  can be estimated by a deconvolution approach.

To realize the fine shift of the exposure, we adopt inserting an existing delay circuit to delay the light emission as shown in Fig. 3. Delaying the light emission is equivalent to reversely shifting the exposure, hence the shift of the exposure is easily controlled. The circuit delays the synchronization signal in sub-nanosecond, hence we can recover high-resolution PSF by a deconvolution approach.

## 2.4 Numerical implementation

The observation  $i_j$  at  $j$ -th delay setting is given by

$$i_j = \int g_j(s) ((l \otimes r)(s)) ds, \quad (7)$$

where  $g_j$  is the  $j$ -th exposure function corresponding to the  $j$ -th delay of light emission. Discretizing Eq. (7),

$$i_j = \mathbf{g}_j^T \mathbf{L} \mathbf{r}, \quad (8)$$

where  $\mathbf{g}_j$  is a vector representing  $j$ -th exposure,  $\mathbf{L}$  is a convolution matrix of emitted wave, and  $\mathbf{r}$  is a vector of discretized temporal PSF, whose resolution is the same as the width of the delay.

Superposing all the observations,

$$\mathbf{i} = \mathbf{G} \mathbf{L} \mathbf{r}, \quad (9)$$

where

$$\begin{cases} \mathbf{i} &= [i_1 \quad i_2 \quad \cdots \quad i_m]^T \\ \mathbf{G} &= [\mathbf{g}_1^T \quad \mathbf{g}_2^T \quad \cdots \quad \mathbf{g}_m^T]^T, \end{cases} \quad (10)$$

and  $m$  is the number of observations.

Since both the exposure setting and the emission waveform are known, the matrix  $\mathbf{G} \mathbf{L}$  is a known matrix. Therefore, if the number of the observation is sufficiently large, the temporal PSF  $\mathbf{r}$  can be estimated by the least squares method as

$$\mathbf{r} = (\mathbf{G} \mathbf{L})^+ \mathbf{i}, \quad (11)$$

where  $(\mathbf{G} \mathbf{L})^+$  is the pseudo-inverse matrix.

In practice, matrix  $\mathbf{G} \mathbf{L}$  is ill-conditioned like sensor-shift based super-resolution [7] hence the calculation as shown in Eq. (11) is unstable. However, using the property that the intensity of light does not have a negative value, it is expected to estimate robustly against the instability of calculation. The temporal PSF can be estimated by the least square method with the non-negative constraint as

$$\underset{\mathbf{r}}{\operatorname{argmin}} \quad \|\mathbf{i} - \mathbf{G} \mathbf{L} \mathbf{r}\|_2^2 \quad \text{s.t.} \quad \mathbf{r} \succeq 0. \quad (12)$$

Since Eq. (12) is a convex optimization problem, the optimal solution can be obtained in a polynomial time.

### 3. Experiments

We confirm the effectiveness of our method via real-world experiments. We build a measurement system as shown in Fig. 4. A delay circuit as shown in (c), where DS1023 IC (Maxim Integrated) and Arduino micro-controller are equipped, is inserted between a ToF camera S11963-01CR (Hamamatsu Photonics) and the light source. The delay circuit controls the delay of synchronization signal in steps of 0.25 nanoseconds from the computer. Using this system, we obtain multiple images by changing the delay by 0.25 nanosecond steps.

We measure a scene including wood, wax, soap, and

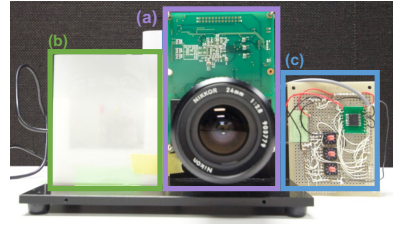


**Fig. 4** Experimental setting. (a) The ToF camera. (b) Light source. (c) Delay circuit with controller.

books as shown in Fig. 5 (a), which cause subsurface scattering and inter-reflection. Firstly, we confirm the effectiveness of the non-negative constraint. Figure 5 (b) shows raw observation corresponding to the low-resolution PSF, estimated PSF by pseudo-inverse, and estimated PSF by non-negative least squares of the wood region. The observation is quite blurred due to the convolution effect of the width of light pulse and exposure time. While pseudo-inverse estimation is suffered from over-fitting, estimated result with the non-negative constraint is more stable, and the effectiveness of non-negative constraint is confirmed. We plot the PSFs of different translucent objects in the detailed scale in Fig. 5 (c). Different shapes of PSFs are estimated, especially for wood and the others. The temporal spread of light inside translucent objects finished within 1 nanosecond, hence our sub-nanosecond estimation have an advantage. Secondly, we recover the temporal PSFs for all pixels as shown in Fig. 5 (d). This is so called ‘light-in-flight’ images and shows how the light propagates in the scene.

We also measure another scene as shown in Fig. 6 (a), which consists of a screen and a mannequin. Figure 6 (b) shows a captured image with long exposure, where the reflection on the screen and the mannequin are superposed. Recovered PSF is shown in Fig. 6 (c), where two peaks are confirmed. The interval of these two peaks is approximately 12 nanoseconds, which correspond to 180cm, and consistent to the distance between the screen and the mannequin. Separating two peaks of the estimated PSF, reflections on the screen and mannequin can be separated as shown in Figs. 6 (d) and (e). Two layers are clearly separated and the sharpened image of the mannequin is obtained.

### 4. Conclusion

In this paper, we propose a method to estimate temporal PSFs with high temporal resolution by combining a pulsed ToF camera and a simple delay circuit. We use the delay circuit to control the light emission timing in units of sub-nanoseconds and recover the temporal PSF by least

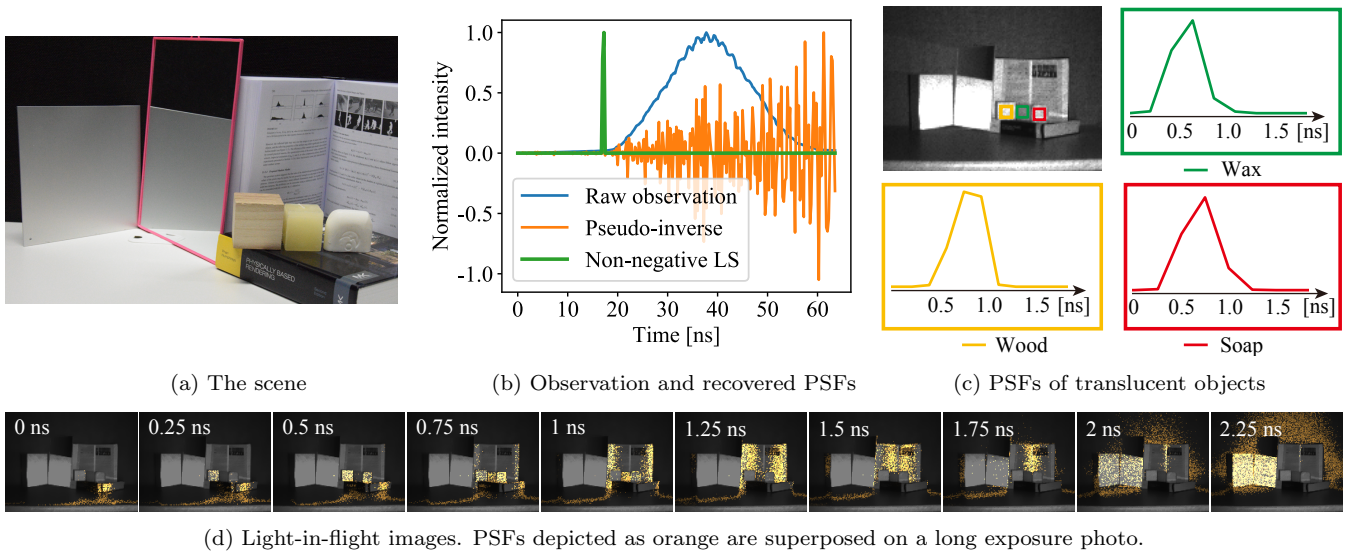


Fig. 5 Experimental result.

(a) The scene. (b) Comparison with observation and recovered results with and without non-negative constraint. Non-negativity contributes to the stability. (c) PSFs of different translucent objects. Different shape of PSFs are recovered. (d) Recovered PSFs for all pixels, as known as light-in-flight images. Light propagation of the scene can be visualized.

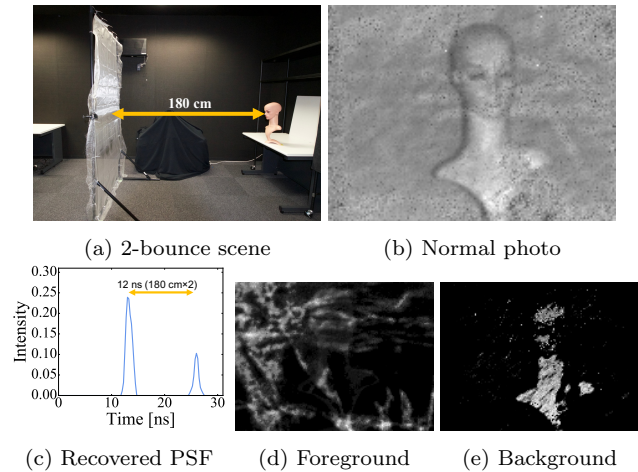


Fig. 6 Result for a mannequin's scene. (a) A mannequin is placed behind the screen. (b) Normal photo. Reflections on the mannequin and the screen is superposed. (c) Recovered PSF has two peaks. (d) Foreground reflection components (reflection of the screen). (e) Background components (Reflection on the mannequin).

square method with the non-negative constraint. We have conducted some real-world experiments and confirm the effectiveness of our method. We are interested in improving more higher temporal resolution in the future research so that the subsurface scattering can be fully analyzed.

**Acknowledgements**

A part of this work was supported by JSPS KAKENHI Grant Number JP15H05918.

**References**

- [1] Gkioulekas, I., Levin, A., Durand, F. and Zickler, T.: Micron-Scale Light Transport Decomposition using Interferometry, *ACM Transactions on Graphics (ToG)*, Vol. 34, No. 4, pp. 37:1–37:14 (2015).
- [2] Heide, F., Hullin, M. B., Gregson, J. and Heidrich, W.: Low-Budget Transient Imaging using Photonic Mixer Devices, *ACM Transactions on Graphics (ToG)*, Vol. 32, No. 4, pp. 45:1–45:10 (2013).
- [3] Kadambi, A., Whyte, R., Bhandari, A., Streeter, L., Barsi, C., Dorrington, A. and Raskar, R.: Coded Time of Flight Cameras: Sparse Deconvolution to Address Multipath Interference and Recover Time Profiles, *ACM Transactions on Graphics (ToG)*, Vol. 32, No. 6, pp. 167:1–167:10 (2013).
- [4] Kakue, T., Tosa, K., Yuasa, J., Tahara, T., Awatsuji, Y., Nishio, K., Ura, S. and Kubota, T.: Digital Light-in-Flight Recording by Holography by Use of a Femtosecond Pulsed Laser, *IEEE Journal of Selected Topics in Quantum Electronics*, Vol. 18, No. 1, pp. 479–485 (2012).
- [5] O’Toole, M., Heide, F., Xiao, L., Hullin, M. B., Heidrich, W. and Kutulakos, K. N.: Temporal Frequency Probing for 5D Transient Analysis of Global Light Transport, *ACM Transactions on Graphics (ToG)*, Vol. 33, No. 4, pp. 87:1–87:11 (2014).
- [6] Peters, C., Klein, J., Hullin, M. B. and Klein, R.: Solving Trigonometric Moment Problems for Fast Transient Imaging, *Proc. ACM SIGGRAPH Asia*, Vol. 34, No. 6, pp. 220:1–220:11 (2015).
- [7] Sung, P., Min, P. and Kang, M.: Super-Resolution Image Reconstruction, *IEEE Signal Processing Magazine*, Vol. 20, No. 3, pp. 21–36 (2003).
- [8] Velten, A., Raskar, R., Wu, D., Jarabo, A., Masia, B., Barsi, C., Joshi, C., Lawson, E., Bawendi, M. and Gutierrez, D.: Femto-Photography: Capturing and Visualizing the Propagation of Light, *ACM Transactions on Graphics (ToG)*, Vol. 32, No. 4, pp. 44:1–44:8 (2013).